

Magnetospheric electric fields from ion data

E. C. Whipple,¹ D. L. Starr,¹ J. S. Halekas,² J. D. Scudder,³ R. D. Holdaway,³ J. B. Faden,³ P. Puhl-Quinn,³ N. C. Maynard,⁴ C. T. Russell⁵

Abstract. We have obtained the magnetospheric electric potential distribution along the path of Polar using ion data from Hydra and magnetic field data from MFE. We used the technique described by Whipple *et al.* [1998] to identify ion drift paths that intersected the spacecraft path at two different locations and times. The difference in energy of the ions at the two times, under certain restrictive assumptions, indicates the potential difference between the two locations. We did this for five minute intervals over 1.5 hours and summed these differences to obtain the potential variation along the spacecraft path. The results agree well with that obtained by the Polar Electric Field Instrument, and are consistent with a co-rotation potential plus a small tailward field of magnitude 0.10 mV/m. This technique can complement and aid in the interpretation of other electric field data, or provide electric field data where such instruments are not available.

1. Introduction

The magnetospheric electric field is an important quantity for magnetospheric processes, but it is difficult to measure. It is important as the driving force for low energy particle convection, and as the only force able to accelerate charged particles to high energies. The drift velocity caused by the electric field perpendicular to the magnetic field is the dominant drift mechanism for charged particles with energies up to a few tens of keV. Drifts due to magnetic field gradients dominate above these energies. Electric fields parallel to the magnetic field have been shown to be important for the acceleration of auroral charged particles. Electric fields in thin current sheets where adiabatic behavior breaks down, as at the magnetopause or in the magnetospheric tail, can accelerate particles to very high energies.

Electric fields have been measured by spacecraft in the ionosphere by sensing the drift velocity of ions with

instruments such as ion traps [Hanson *et al.*, 1993]. Direct measurements of electric fields have been carried out using probes on extended spacecraft booms [Maynard, 1998]. The probes can be isolated electrically and allowed to float to an equilibrium potential. The difference in potential between two probes can then give the potential difference between them and thus the electric field. Biasing the probes with a current which approximates the photoemission current allows the measurement to be made in tenuous plasmas [Pedersen *et al.*, 1998]. A new technique uses a charged particle beam and senses the drift of the particles over one or more gyro-periods. This has been used successfully on the GEOS, Freja, and Equator-S missions, and is planned for the Cluster mission [Paschmann *et al.*, 1997; Kletzing *et al.*, 1998]. These electric field measurements can be integrated to get the potential variations along spacecraft trajectories and then used to form maps of potential distributions [e.g., Weimer, 1996].

Typical electric field magnitudes in the magnetosphere are on the order of tenths to a few mV/m (V/km) during quiet times, and as large as several hundred mV/m during active times [e.g., Markland *et al.*, 1994]. Each of the above techniques for measuring electric fields suffers from perturbations of various sorts. The difficulties are primarily due to the smallness of the field and the susceptibility to other effects, such as lack of symmetry between probes (for the probe technique), difficulty in targeting the detectors (for the beam technique), etc. Any new way of obtaining information on the magnetospheric electric field would be of great value in complementing and interpreting data from these present methods.

We have recently shown how to identify charged particles that travel between pairs of spacecraft in the magnetosphere [Whipple *et al.*, 1998]. The difference in the particle energies at the two spacecraft is a measure of the magnetospheric potential difference, and thus this technique enables a connection to be made between the mapping of potential distributions by different spacecraft. The purpose of this paper is to show that it is possible to extend this technique and to use it on a single spacecraft to obtain the potential variation along the spacecraft path from particle data.

2. Summary of Analysis Technique

The assumptions made in this work are: (1) Particle paths are without collisions and with negligible sources or sinks so that Liouville's theorem is valid. (2) Steady-

¹Geophysics Program, University of Washington, Seattle, Washington.

²University of California, Berkeley, California.

³University of Iowa, Iowa City, Iowa.

⁴Mission Research Corporation, Nashua, New Hampshire.

⁵Institute of Geophysics and Planetary Physics, University of California at Los Angeles.

state conditions exist so that inductive electric fields are negligible and the velocity distributions are independent of position along a particle path. (3) Parallel electric fields are negligible and so field lines are equipotentials. (4) The Tsyganenko [1995] magnetic field model is reasonably accurate over the studied region.

The analysis scheme for identifying particles that travel between two different spacecraft was described in Whipple *et al.* [1998]. We adapt that scheme to a single spacecraft with data at two different times. We use the Tsyganenko [1995] magnetic field model to map the pitch angles of particles that could travel between the two locations. This mapping depends only on the magnetic field and is independent of particle species and energy. The magnetic moment μ determines where the particle mirrors on a field line, and the modified longitudinal invariant K [Kaufmann, 1965] determines the surface in space on which the particle mirrors, $K(\mathbf{r}) = \oint \sqrt{B(\mathbf{r}) - B(s)} ds = J/\sqrt{2e\mu}$, where $J = \oint m\mathbf{v}_{\parallel} ds$ is the ordinary longitudinal invariant. $K(\mathbf{r})$ is itself independent of any particle property, but a particle that mirrors at \mathbf{r} has its mirror point drift on that constant $K(\mathbf{r})$ surface. If the particle drifts between the field lines which the spacecraft intercepts at the two times (whether it does or not does depend on the particle energy), then the magnetic field at the mirror points on those field lines determines the pitch angles at the spacecraft at those times.

Conservation of μ and total energy at times 1 and 2 yield:

$$\frac{E_2}{E_1} = \frac{B_2(K)}{B_1(K)} \quad (1)$$

$$E_2 - E_1 = -e\Delta U \quad (2)$$

The magnetic field model yields a relation between pitch-angles (subscript "o" means at Polar):

$$\sin^2 \alpha_{1o} = \frac{B_{1o}}{B_1(K_i)}, \quad \sin^2 \alpha_{2o} = \frac{B_{2o}}{B_2(K_i)} \quad (3)$$

E is kinetic energy and ΔU is the potential difference between the field lines. There are two equations for the three unknowns: E_1 , E_2 and ΔU . To close the system we invoke Liouville's theorem which states that particle phase space densities are constant along a particle path in a collisionless environment. We search in energy at the two pitch angles determined by the mirror point surface K . We perform a chi-squared test on the differences in the (logarithm of) distribution functions summed over K , for a systematic set of guesses for ΔU . A minimum in χ^2 identifies the appropriate ΔU .

3. Data Selection

We work with data from the Hydra plasma instrument on Polar [Scudder *et al.*, 1995] and with the magnetic field data from the Magnetic Field Experiment [Russell *et al.*, 1995]. We have selected a time period for analysis from 18:30 - 20:00 UT on 3/04/97.

During this time the Polar satellite was coming down

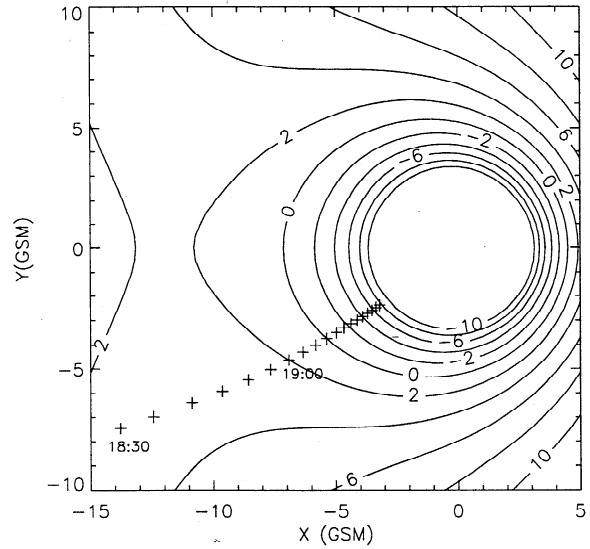


Figure 1. Trajectory of Polar from 18:30 to 20:00 on March 4, 1997. The positions of the magnetic field lines which Polar is crossing are shown where the field lines intersect the GSM equator, at five minute intervals. The contours are equipotentials, in kV, of the model potential distribution (see section 5).

from apogee on the night side of the earth towards the earth's equator. At 18:30 its altitude above the GSM equator was $3.52 R_E$; at 19:15 it was $2.05 R_E$, and at 20:00 it was $0.43 R_E$. At 19:08 it crossed the field line which intersects the earth's equator at synchronous altitude. Fig. 1 shows the GSM equatorial position of the magnetic field lines on which Polar was situated at five minute intervals during this time. It also shows equipotential contours for the potential distribution consistent with our results (section 5). The magnetospheric activity levels were reasonably low. DST changed from -17.5 to -19.0 nT, and the K_p index was 1.

4. A Sample Analysis

We show some details of the analysis for the time interval from 19:00 - 19:05. We first chose a set values for K , in this case from $K = 300$ to $2000 \sqrt{nT} R_E$ at intervals of 100. This set of K_i determined a set of pitch-angles at each spacecraft according to (3). We then chose values for ΔU , from 0 to -2 kV in -10 V steps. At each value for ΔU we used (1) and (2) to find E_1 and E_2 for each value of K_i . We then found the ion distribution functions $f_1(\mathbf{v}_{1i})$ and $f_2(\mathbf{v}_{2i})$ from the Hydra data, where the vectors \mathbf{v}_{1i} and \mathbf{v}_{2i} are the velocities associated with the two sets of energies and pitch-angles from the set of K_i . This involved fitting $(\log f)$ to pitch-angles at each instrument energy and then interpolating to obtain $f(\mathbf{v}_{i,j})$.

At each ΔU we formed: $\Delta LF_j = \sum_i [\log(f_1(\mathbf{v}_{1i,j})) - \log(f_2(\mathbf{v}_{2i,j}))]$, where i refers to the selected energy and pitch-angle as described above, and j refers to the j th ΔU . We also form the chi-squared sum: $\chi_j^2 = \sum_i [\log(f_1(\mathbf{v}_{1i,j})) - \log(f_2(\mathbf{v}_{2i,j}))]^2 / [\sigma(i,j)]^2$, where σ is

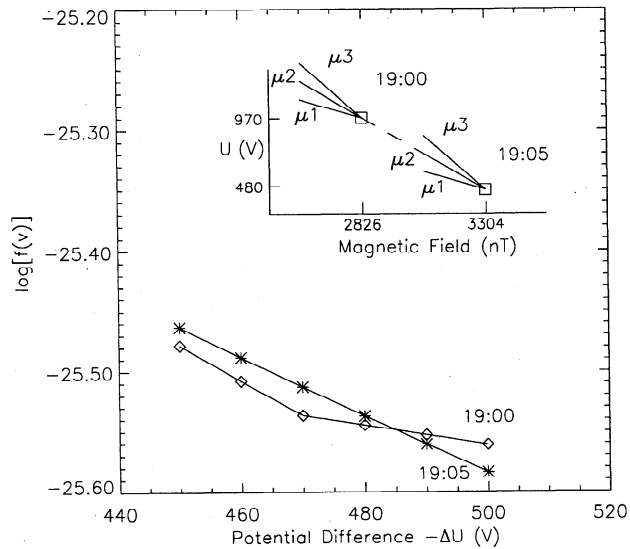


Figure 2. Illustration using (U, B) coordinates in $K = 1500\sqrt{nTR_E}$ surface showing why the distribution functions at two times should cross as ΔU progresses through the correct value. As $(-\Delta U)$ increases, the energy and thus the slope (proportional to μ) increases in magnitude. The middle slope (μ_2) defines the drift path that connects the two locations. The inset shows interpolated values of $(\log f)$ as a function of ΔU on the same K -surface at 19:00 and 19:05.

the appropriate joint standard deviation for the logarithms of the two measurements of $f(\mathbf{v})$. We have selected the following criteria for choosing that ΔU which we believe to be the best value for ΔU between the two spacecraft locations. We look for the deepest minimum in χ_j^2 as a function of ΔU that is associated (i.e. at or near the same ΔU) with a zero-crossing of ΔLF_j , and designate that value as the correct potential difference. If there is no associated zero-crossing of ΔLF_j then we choose the deepest minimum in χ_j^2 . For the time interval from 19:00-19:05 the χ^2 test gave a value for ΔU of -490 V, with $\chi^2 \cong 0.01$ at the minimum.

The reason we look for an associated zero-crossing of ΔLF_j is illustrated in the inset of Fig. 2, where we have plotted the positions of the two spacecraft at the two times in (U, B) coordinates in a constant K surface. The drift paths of particle mirror points are straight lines, with a slope of $(-\mu/e)$ [Whipple, 1978]. But this slope is given by $(\Delta U/\Delta B)$ where $\Delta B = B_2(K) - B_1(K)$ is 478 nT. We show three pairs of drift paths converging on the two spacecraft, each pair with the same slope. The middle path goes through both spacecraft and has the correct slope, given by $(-\mu/e) = (\Delta U/\Delta B) = (-490 \text{ V}/478 \text{ nT}) = -1.025 \text{ V/nT}$.

5. Results for the Potential Distribution

We have summed the inferred values of ΔU for every five-minute interval between 18:30 and 20:00, and

then subtracted from the cumulative sum the value at 19:15 to normalize the potential distribution so that it goes through zero at that time. This result is shown as the solid curve in Fig. 3. The dashed curve is the result from the Electric Field Instrument (EFI) on Polar [Harvey *et al.*, 1995], normalized in the same way since the absolute value of the potential is arbitrary. It is the slope of the two curves that are significant, since they represent the electric field component along the spacecraft path. The slopes of the two curves are in reasonable agreement, with the differences between them having the same order of magnitude as the fluctuations in either curve.

We show two other sets of symbols in Fig. 3: the set of plus signs show a model potential given by the corotation electric field with a uniform superimposed tailward field. This is in the negative x -direction but with a small value of only 0.10 mV/m. This model potential agrees reasonably with the two measured distributions. The seven asterisks located at 15 minute intervals represent measurements of ΔU from Hydra data between 15 minute locations of Polar, starting at 18:30, and then summed and normalized to the cumulative value at 19:15. These also show consistency with the other potential distributions.

6. Conclusions

We conclude that it is possible to use charged particle data from a single spacecraft to obtain valid magnetospheric electric field information. In particular it is possible to obtain the potential variation along the spacecraft path during quiet times. This capability should be a useful additional tool for obtaining information on the magnetospheric electric field, especially on spacecraft which do not carry an electric field instrument. But even with such an instrument the ability to acquire additional information could be quite useful.

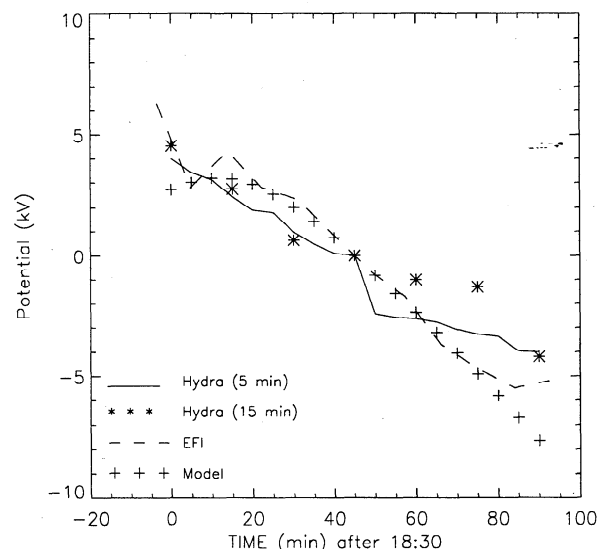


Figure 3. Potential distribution along the path of the Polar satellite from 18:30 to 20:00.

The separation of the locations of Polar for these 5-minute intervals was a few hundred km, which is similar to the planned separation of the 4 Cluster spacecraft. This technique should be a valuable tool for connecting electric field measurements made by these spacecraft.

We have returned to the data that we analyzed in our earlier paper [Whipple et al., 1998] and used this "single spacecraft" technique to acquire the potential variation, $U(s)$, along the paths of both Polar and Geotail during the analysis time. We confirmed the $U(s)$ for Geotail obtained from the electric field detector, EFD, using data from the Comprehensive Plasma Instrument, and also $U(s)$ for Polar obtained from EFI on Polar for the time from 18:30 to 19:00. But we obtained a slightly different $U(s)$ for 18:00 to 18:30 so that the new potential at 18:00 after normalization was -6 kV instead of -8 kV (see Fig. 11 in that paper). This gave a more consistent agreement with the inferred potential differences between the two spacecraft (we mentioned in that paper that the Polar EFI measurements were questionable before 18:15).

We note that even if there were a time-dependent, inductive electric field, Liouville's theorem remains valid and so this analysis should still obtain the integral of the electric field along the spacecraft path, although such a non-conservative field may not be interpretable in terms of a potential distribution. This would give the gain in energy of a particle drifting between the two spacecraft locations, as long as parallel electric fields were insignificant. Present particle instruments have such high sensitivity and resolution in time, energy, and direction, that we believe significant quantitative information on magnetospheric transport processes can be extracted as we have done here.

Acknowledgments. We thank T. G. Northrop for helpful discussions, and G. Parks for his support through NASA space grant NGT5-40017 at the University of Washington. The work was also partially supported by NASA grant NA5-4686. The results of this paper were made possible by Hydra NASA funding under grant NAG 5-2231 to the University of Iowa, and DARA grant 50-OC 8911-0. The present results of the Hydra investigation would not have been possible without the decade-long hardware efforts led at NASA GSFC by K. Ogilvie, at UNH by R. Torbert, at MPI Lindau by A. Korth, and at UCSD by W. Fillius. The work at UCLA was supported by NASA grant NAG5-3171, and at Mission Research Corporation by NASA through UCB under grants NAS5-30367 and NAG5-3182.

References

- Gustafson, G., et al., The electric field and wave experiment for the Cluster mission, *Spa. Sci. Rev.*, 79, 137-156, 1997.
- Hanson, W. B., et al., A comparison of in situ measurements of \vec{E} and $-\vec{v} \times \vec{B}$ from Dynamics Explorer 2, *J. Geophys. Res.*, 98, 21501, 1993.
- Harvey, P., et al., The electric field instrument on the Polar satellite, *Spa. Sci. Rev.*, 71, 583-596, 1995.
- Kaufmann, R. L., Conservation of the first and second adiabatic invariants, *J. Geophys. Res.*, 70, 2181-2186, 1965.
- Kletzing, C. A., G. Paschmann, and M. Boehm, Electric field measurements using the electron beam technique at low altitudes, *Measurement Techniques in Space Plasmas: Fields*, edited by R. Pfaff et al., pp. 53-58, Geophysical Monograph 103, AGU, Washington, D. C., 1998.
- Markland, G., et al., On intense diverging electric fields associated with black aurora, *Geophys. Res. Lett.*, 21, 1859-1862, 1994.
- Maynard, N. C., Electric field measurements in moderate to high density space plasmas with passive double probes, *Measurement Techniques in Space Plasmas: Fields*, edited by R. Pfaff et al., pp. 13 - 27, Geophysical Monograph 103, AGU, Washington, D. C., 1998.
- Paschmann, G., et al., *Spa. Sci. Rev.*, The Electron Drift Instrument for Cluster, *Spa. Sci. Rev.*, 79, 233-269, 1997.
- Pedersen, A., F. Mozer, and G. Gustafson, in *Electric Field Measurements in a Tenuous Plasma with Spherical Double Probes*, *Measurement Techniques in Space Plasmas: Fields*, edited by R. Pfaff et al., pp. 1-12, Geophysical Monograph 103, AGU, Washington D.C., 1998.
- Russell, C. T., et al., The GGS/Polar magnetic fields investigation, *Spa. Sci. Rev.*, 71, 563-582, 1995.
- Scudder, J., et al., Hydra—a 3-dimensional electron and ion hot plasma instrument for the Polar spacecraft of the GGS mission, *Spa. Sci. Rev.*, 71, 459-495, 1995.
- Tsyganenko, N. A., Modeling the Earth's magnetospheric magnetic field confined within a realistic magnetopause, *J. Geophys. Res.*, 100, 5599-5612, 1995.
- Weimer, D. R., A flexible IMF dependent model of high-latitude electric potentials having "space weather" applications, *Geophys. Res. Lett.*, 23, 2549-2552, 1996.
- Whipple, E. C., (U, B, K) coordinates: a natural system for studying magnetospheric convection, *J. Geophys. Res.*, 83, 4318-4326, 1978.
- Whipple, E. C., et al., Identification of magnetospheric particles that travel between spacecraft and their use to help obtain magnetospheric potential distributions, *J. Geophys. Res.*, 103, 93-102, 1998.
- J. S. Halekas, University of California, Berkeley, 94720.
- N. C. Maynard, Mission Research Corp., Nashua, NH, 03062.
- C. T. Russell, UCLA, Los Angeles, CA 90024.
- J. D. Scudder, R. D. Holdaway, J. B. Faden, P. Puhl-Quinn, University of Iowa, Iowa City, IA, 52242.
- E. C. Whipple and D. L. Starr, Geophysics Program, University of Washington, P. O. Box 351650, Seattle, WA 98195. (e-mail: whipple@geophys.washington.edu)

(Received January 22, 1999; revised April 12, 1999; accepted April 14, 1999.)